



# Splinter vortices at inhomogeneous asymmetric grain boundaries in YBCO films

R.G. Mints \*, Ilya Papiashvili

*School of Physics and Astronomy, Raymond and Beverly Sackler Faculty of Exact Sciences, Tel Aviv University, Tel Aviv 69978, Israel*

Received 1 September 2003; received in revised form 15 December 2003; accepted 18 December 2003

## Abstract

We consider both analytically and numerically the effect of inhomogeneity of Josephson properties of grain boundaries in YBCO thin films on unquantized (splinter) vortices. It is shown that in general a smooth inhomogeneity breaks the complementarity condition  $\phi_1 + \phi_2 = \phi_0$  relating magnetic fluxes  $\phi_1$  and  $\phi_2$  carried by adjacent splinter vortices.

© 2003 Elsevier B.V. All rights reserved.

PACS: 74.60.Ec; 74.60.Ge

Keywords: YBCO; Grain boundaries; Vortices

## 1. Introduction

The recent observation of spontaneous flux structures at asymmetric grain boundaries in  $\text{YBa}_2\text{Cu}_3\text{O}_{7-x}$  thin films reveals fragments with unquantized vortices (*splinter* vortices) [1]. This observation is a notable exhibition of unusual Josephson properties of these grain boundaries.

A consistent understanding of the spatial structure of the spontaneous flux [2,3] located at the asymmetric grain boundaries in  $\text{YBa}_2\text{Cu}_3\text{O}_{7-x}$  involves into consideration the  $d_{x^2-y^2}$  wave symmetry component of the superconducting order parameter [4–12] and the fine-scale faceted struc-

ture of the grain boundaries [8,13–16]. These two well established facts are of a special importance for the asymmetric  $45^\circ$  [001]-tilt grain boundaries in  $\text{YBa}_2\text{Cu}_3\text{O}_{7-x}$  thin films. In this case the combined effect of the d-wave symmetry and faceting results in Josephson's critical current density  $j_c(x)$  alternations along the grain boundary line ( $x$ -axis). The typical length-scale  $l$  (facets size) of these alternations is of the order of 10–100 nm and the average  $\langle j_c(x) \rangle$  is almost zero [17].

The spatial alternations of  $j_c(x)$  is the physical reason of the spontaneous flux arising at the grain boundaries in YBCO thin films [2]. It has been predicted theoretically that if  $j_c(x)$  is periodic, then the spontaneous flux patterns may include fragments consisting of pairs of splinter vortices carrying unquantized fluxes  $\phi_1, \phi_2$  [3]. The values of  $\phi_1$  and  $\phi_2$  obey the complementarity condition

\* Corresponding author. Tel.: +972-3-6409165; fax: +972-3-6422979.

E-mail address: [mints@post.tau.ac.il](mailto:mints@post.tau.ac.il) (R.G. Mints).

$$\phi_1 + \phi_2 = \phi_0, \quad (1)$$

where  $\phi_0$  is the flux quantum,  $\phi_1 \leq \phi_0/2$  and  $\phi_2 \geq \phi_0/2$ .

The recent observation of the splinter vortices [1] confirmed the basic theoretical results. At the same time it follows from the experimental data that the flux carried by a pair of adjacent splinter vortices does not necessarily match the complementarity condition. This mismatch is an important fundamental problem which has to be solved in order to have a comprehensive understanding of flux patterns caused by the spatial alternations of  $j_c(x)$  along grain boundaries in YBCO films [2], zigzag-shaped Josephson junctions between YBCO and Nb [18], etc.

We claim that the broken complementarity condition is caused by spatial variations of the facets size  $l(x)$  and the amplitude of alternations of  $j_c(x)$ , this amplitude we define as one half of the absolute value of the peak-to-peak difference of  $j_c(x)$  values.

In this paper we report on analytical and numerical analysis of flux patterns including fragments with broken complementarity condition for adjacent splinter vortices [19]. Specifically, we treat the effect of smooth inhomogeneities of the facets size  $l(x)$  and amplitude of alternations of  $j_c(x)$  on the fluxes carried by the splinter vortices. In other words we assume that the values of  $l(x)$  and amplitude of  $j_c(x)$  alternations vary slightly along a grain boundary with a typical length scale  $L \gg A_J$  (*smooth* variation), where  $A_J$  is of the order of a splinter vortex length given by the effective Josephson length [3]

$$A_J = \sqrt{\frac{c\phi_0}{16\pi^2\lambda\langle j_c(x) \rangle}} \quad (2)$$

and  $\lambda$  is the London penetration depth.

Our qualitative and quantitative studies demonstrate that the smooth inhomogeneities lead to a dependence of the fluxes  $\phi_1$  and  $\phi_2$  on the splinter vortices location. This, in general, breaks the complementarity condition and allows for existence of adjacent splinter vortices carrying a certain flux  $\phi_s$  less than the flux quantum  $\phi_0$ . The value of  $\phi_s$  depends significantly on the location of

the splinter vortex. It is also worth noting that the inhomogeneities under consideration have to be weak enough not to destroy the correlated state which is the background for splinter vortices and strong enough to break the complementarity condition.

The organization of the paper is as follows. First, we review briefly the flux patterns developed by a periodically alternating Josephson critical current density  $j_c(x)$  [3]. Using the two-scale perturbation approximation we find the fluxes  $\phi_1$  and  $\phi_2$  in the form which allows for a qualitative analyzes of the effect of smooth inhomogeneities of the facets size  $l(x)$  and of the amplitude of alternations of  $j_c(x)$  on the splinter vortices. Second, we demonstrate the main results of our numerical simulations of the spontaneous flux patterns at the grain boundaries with  $j_c(x)$  having a smoothly varying amplitude of alternations and period  $l(x)$ . The results of these numerical simulations are in a good qualitative agreement with the flux patterns that were recently observed for the splinter vortices [1]. Finally, we summarize briefly the obtained results.

## 2. Splinter vortices

Consider a plain asymmetric  $45^\circ$  [0 0 1]-tilt grain boundary in a superconducting  $\text{YBa}_2\text{Cu}_3\text{O}_{7-x}$  film. We model this grain boundary by an ideal one-dimensional Josephson junction with a periodically alternating critical current density  $j_c(x)$  [3]. It is convenient to write  $j_c(x)$  as

$$j_c = \langle j_c \rangle [1 + g(x)], \quad (3)$$

where  $\langle j_c \rangle$  is the average value of the critical current density, the dimensionless function  $g(x)$  alternates with a period  $l$  and has a zero average:  $\langle g(x) \rangle = 0$ . The phase difference across a grain boundary  $\varphi(x)$  then satisfies

$$A_J^2 \varphi'' - [1 + g(x)] \sin \varphi = 0. \quad (4)$$

It follows from the experimental data [1,2] that the typical value of the effective Josephson length  $A_J \sim 10 \mu\text{m}$ , i.e.,  $l \ll A_J$ . This means that the problem under consideration has two very different length scales and thus can be effectively treated

in the framework of the two-scale perturbation theory [20,21]. In this approach, we write the total phase difference  $\varphi(x)$  as a sum  $\varphi(x) = \psi(x) + \xi(x)$ , where the smooth phase  $\psi(x)$  has a length scale  $A_J$  and the fast alternating phase  $\xi(x)$  has a length scale  $l$  and a small amplitude  $|\xi(x)| \ll 1$ . As a result we have for the phases  $\psi(x)$  and  $\xi(x)$  the following equations [3]:

$$A_J^2 \psi'' - \sin \psi + \gamma \sin \psi \cos \psi = 0, \quad (5)$$

$$\xi(x) = \xi_g(x) \sin \psi, \quad (6)$$

where the function  $\xi_g(x)$  and parameter  $\gamma$  are defined by

$$A_J^2 \xi_g'' = g(x), \quad (7)$$

$$\gamma = -\langle g(x) \xi_g(x) \rangle = A_J^2 \langle \xi_g'^2 \rangle > 0. \quad (8)$$

The value of  $\gamma$  depends only on the spatial distribution of  $j_c(x)$  and thus characterizes individual Josephson properties of a particular grain boundary. It is also worth mentioning that the two-scale approach is valid only if  $j_c(x)$  is a periodic function [21]. A spontaneous flux pattern at a grain boundary with a randomly alternating  $j_c(x)$  is very complicated and can be treated only numerically.

A single Josephson vortex is described by a solution of Eq. (5) matching the two standard boundary conditions  $\psi'(\pm\infty) = 0$ . Using Eq. (5) these two conditions transform into  $\sin \psi_{\pm}(1 - \gamma \cos \psi_{\pm}) = 0$ , where  $\psi_{\pm} = \psi(\pm\infty)$  and the flux carried by a vortex is  $\phi = \phi_0(\psi_+ - \psi_-)/2\pi$ .

If  $\gamma < 1$ , then there is one vortex-type solution ( $\psi_+ = 0, \psi_- = 2\pi$ ), which describes a single Josephson vortex carrying one flux quantum  $\phi_0$ . If  $\gamma > 1$ , then there are two vortex-type solutions describing two splinter vortices. For the first splinter vortex the phase  $\psi(x)$  increases from  $\psi_- = -\psi_\gamma$  to  $\psi_+ = \psi_\gamma$ , where

$$\psi_\gamma = \arccos(1/\gamma), \quad (9)$$

the phase difference is given by  $\psi_+ - \psi_- = 2\psi_\gamma$ , and thus this vortex carries the flux  $\phi_1 = \psi_\gamma \phi_0 / \pi < \phi_0/2$ . For the second splinter vortex we have  $\psi_- = \psi_\gamma, \psi_+ = 2\pi - \psi_\gamma$ , the phase difference is given by  $2\pi - 2\psi_\gamma$ , and thus this vortex carries the flux  $\phi_2 =$

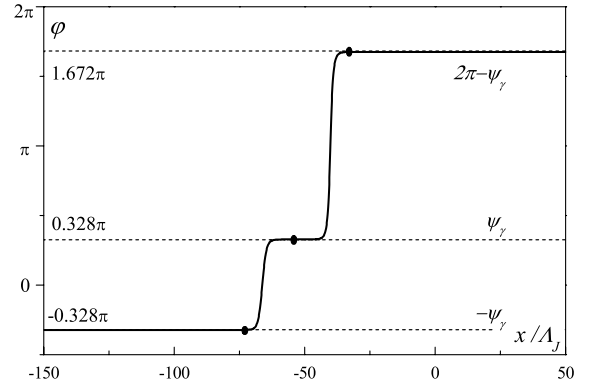


Fig. 1. A phase pattern for a pair of “ideal” splinter vortices located at a grain boundary with a periodic alternating critical current density,  $g_0 = 125$ . The fluxes  $\phi_1 = 0.328\phi_0$  and  $\phi_2 = 0.672\phi_0$  carried by these vortices match the complementarity condition given by Eq. (1).

$(1 - \psi_\gamma/\pi)\phi_0 > \phi_0/2$ . These two splinter vortices are complementary as  $\phi_1 + \phi_2 = \phi_0$ .

In Fig. 1 we show results of our numerical simulations of the main Eq. (4) for the spatial distribution of the phase difference  $\varphi(x)$ . This fragment of the phase pattern  $\varphi(x)$  contains two adjacent “ideal” splinter vortices. The simulations were performed for a model dependence  $g(x) = g_0 \sin(2\pi x/l)$  with  $g_0 = 125$  and  $l = 0.1A_J$ , which results in  $\phi_1 = 0.328\phi_0$  and  $\phi_2 = 0.672\phi_0$  matching the complementarity condition.

### 3. Splinter vortices and smooth inhomogeneities

Assume now that there is a smooth inhomogeneity of the amplitude of the critical current density or/and of the facets size, i.e., both quantities vary along the grain boundary line with a typical length-scale  $L \gg A_J$ . In this case the spontaneous flux patterns are very complicated and the two-scale approximation is valid at the most for a brief qualitative analysis [21]. Moreover, this analysis has to be backed up by thorough numerical simulations of the exact Eq. (4).

If we write the total phase  $\varphi(x) = \psi(x) + \xi(x)$  and average the main Eq. (4) over a certain distance  $\ell$ , where  $L \gg \ell$ . As a result we arrive to the system of Eqs. (5)–(8), where the parameter

$\gamma = \gamma(x)$  varies along the  $x$  axis with a typical length-scale  $L$ .

It follows from the analysis reviewed in the previous section that a spontaneous flux pattern can include the splinter vortices at the grain boundary regions where  $\gamma(x) > 1$ . The simplest fragment of this pattern contains a pair of single splinter vortices with fluxes  $\phi_1(x_1) \leq \phi_0/2$  and  $\phi_0/2 \leq \phi_2(x_2) \leq \phi_0$ , where  $x_1$  and  $x_2$  are the coordinates of the vortices. The phase difference  $\varphi(x)$  generated by these vortices is increasing from  $-\psi_\gamma(x_1)$  to  $\psi_\gamma(x_1)$  for the first vortex and from  $\psi_\gamma(x_2)$  to  $2\pi - \psi_\gamma(x_2)$  for the second vortex. In general, a “dilute” spontaneous flux pattern is a certain sequence of single splinter vortices and antivortices with fluxes  $-\phi_1(x_1)$  and  $-\phi_2(x_2)$ .

If the distance between two adjacent vortices  $l_v$  is much less than  $L$  then the value of the parameter  $\gamma$  is the same for both vortices and the complementarity condition (1) holds locally. Indeed, the flux carried by the two vortices is  $\phi = \phi_1(x) + \phi_2(x + l_v) \approx \phi_1(x) + \phi_2(x) = \phi_0$  within error bars  $|\phi - \phi_0|/\phi_0 \sim l_v/L \ll 1$ . If the distance  $l_v \gtrsim L$ , then the value of the sum of  $\phi_1$  and  $\phi_2$  depends on the inhomogeneity of the Josephson properties of the grain boundary and, in general, is different from the flux quantum  $\phi_0$ , i.e., in this case the condition (1) is broken.

To confirm the above qualitative consideration we perform numerical simulations of the main Eq. (4) using for an alternating critical current density the model dependence  $g(x) = g_0(x) \sin[2\pi x/l(x)]$ . In this case the phase difference across a grain boundary  $\varphi(x)$  satisfies [3]

$$A_J^2 \varphi'' - \{1 + g_0(x) \sin[2\pi x/l(x)]\} \sin \varphi = 0 \quad (10)$$

and the two scale approach applied to Eq. (10) results in the following formula for the parameter

$$\gamma(x) = g_0^2(x) l^2(x) / 8\pi^2 A_J^2 \quad (11)$$

smoothly varying with a typical length scale  $L \gg A_J$ .

First, we use Eq. (10) to consider a grain boundary with a varying amplitude  $g_0(x)$  of the critical current density and with a fixed length of the facets  $l$ . The function  $g_0(x)$  we model as  $g_0(x) = 112.5 + 12.5 \sin(2\pi x/200A_J)$ , which means

that  $100 \leq g_0(x) \leq 125$  and the typical length-scale  $L \sim 100A_J$ . Also, in these numerical simulations we use  $l = 0.1A_J$  and thus  $l \ll A_J \ll L$ .

The results of our numerical simulations are shown in Figs. 2 and 3 for two qualitatively different spatial distributions of the spontaneous flux localized at the same grain boundary (solid and

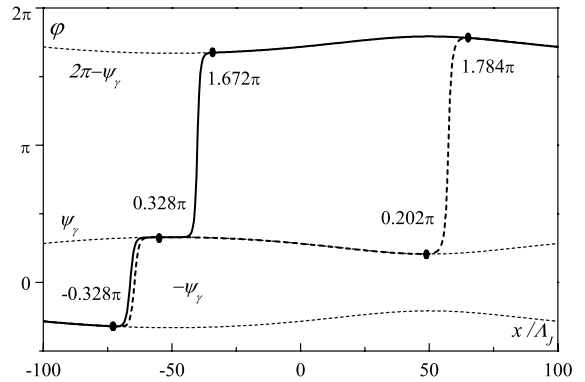


Fig. 2. Two fragments of phase patterns obtained by numerical simulations,  $L \sim 100A_J \gg A_J$ . Three dotted lines depict the reference dependencies  $-\psi_\gamma(x)$ ,  $\psi_\gamma(x)$ , and  $2\pi - \psi_\gamma(x)$ . The solid line shows a pattern with two adjacent splinter vortices separated by  $l_v \approx 25A_J \ll L$ , the fluxes  $\phi_1 = 0.328\phi_0$  and  $\phi_2 = 0.672\phi_0$  match the complementarity condition. The dashed line depicts a pattern with two splinter vortices separated by  $l_v \approx 100A_J \sim L$ , the fluxes  $\phi_1 = 0.328\phi_0$ ,  $\phi_2 = 0.791\phi_0$  do not match the complementarity condition.

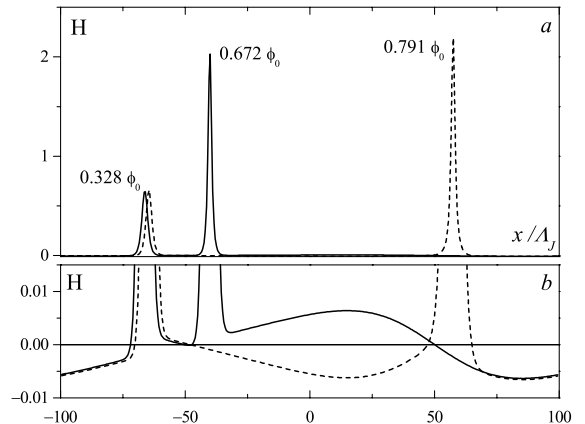


Fig. 3. The spontaneously generated magnetic field  $H(x)$  computed for the phase patterns shown in Fig. 2,  $H \propto d\varphi/dx$ .

dashed lines). The dotted lines in Fig. 2 depict the three reference lines  $-\psi_\gamma(x)$ ,  $\psi_\gamma(x)$ , and  $2\pi - \psi_\gamma(x)$ , where the dependence of the phase  $\psi_\gamma$  on the coordinate  $x$  is a consequence of the dependence  $\gamma(x)$ . The solid line is for the first spontaneous flux spatial distribution  $\varphi(x)$ , which includes two splinter vortices located at a distance  $l_v \ll L$  from each other. The dashed line is for the second spontaneous flux spatial distribution  $\varphi(x)$ , which includes two splinter vortices located at a distance  $l_v \gtrsim L$  from each other. In this case the fluxes  $\phi_1$  and  $\phi_2$  are defined by two different values of  $\gamma$ , i.e.,  $\gamma(x_1)$  and  $\gamma(x_2)$  and therefore, in general, the sum  $\phi_1 + \phi_2$  is not equal to  $\phi_0$ , i.e., the complementarity condition (1) is broken. In Fig. 3 we demonstrate the spatial distributions of the spontaneously generated magnetic field  $H \propto d\varphi/dx$  for the splinter vortices shown in Fig. 2. This figure allows for an accurate measurement of the distance between the vortices.

Next, we use Eq. (10) to consider the effect of the facets length variation on the single splinter vortices. The results of our numerical simulations are shown in Fig. 4 for the case of a grain boundary with  $l(x)$  linearly increasing from  $l = 0.04A_J$  at  $x = 0$  to  $l = 0.14A_J$  at  $x = 500A_J$ . This phase pattern demonstrates the basic features of a sequence of splinter vortices at an asymmetric grain boundary with a smooth inhomogeneity of its Josephson properties. In particular, the splinter vortices appear only at  $x > 100A_J$ , which is the region where  $\gamma(x) > 1$ . In addition, as shown in Fig. 4 the value of  $\phi_1$  decreases from  $\phi_0$  at  $x \approx 100A_J$  to  $0.5\phi_0$  at  $x \approx 500A_J$ , and  $\phi_2$  increases from zero at  $x \approx 100A_J$  to  $0.5\phi_0$  at  $x \approx 500A_J$ , and the complementarity condition holds only for the adjacent vortices at  $x \gtrsim 350A_J$ .

Finally, we treat the splinter vortices at a grain boundary where certain random variations of  $l(x)$  and  $j_c(x)$  are superimposed on smooth variations of  $l(x)$  and  $j_c(x)$ . The phase pattern shown in Fig. 5 is obtained numerically for a grain boundary with a random sequence of the lengths of the facets with a standard deviation  $\delta l = \sqrt{\langle l^2 \rangle - \langle l \rangle^2} = 0.005A_J \ll l(x)$ . This short-range randomness of the dependence  $l(x)$  is superimposed on the smooth dependence  $l(x)$  which

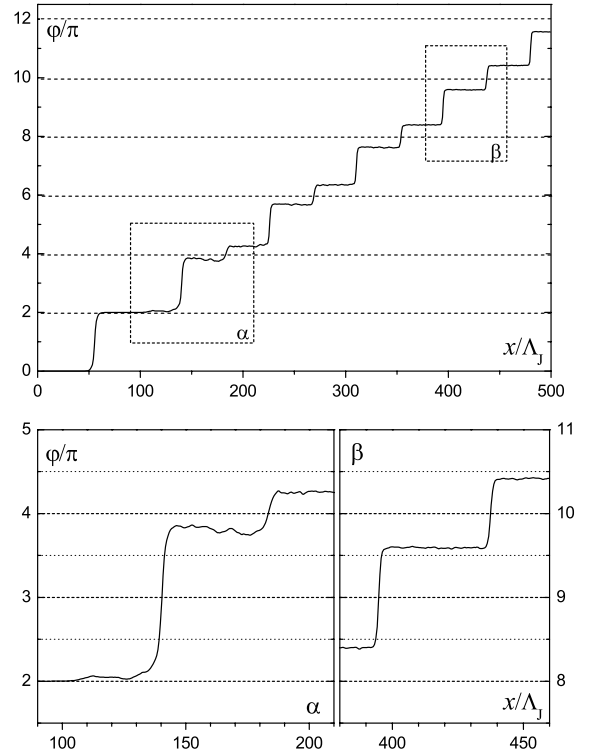


Fig. 4. A fragment of a phase pattern obtained by numerical simulations, the length of the facets  $l(x)$  is linearly increasing from  $l(0) = 0.04A_J$  to  $l(500A_J) = 0.14A_J$ ,  $g_0 = 135$ . The splinter vortices exist for  $x > 100A_J$ , the flux  $\phi_1(x)$  decreases from  $\phi_1(100A_J) = \phi_0$  to  $\phi_1(500A_J) = 0.5\phi_0$  and the flux  $\phi_2(x)$  increases from  $\phi_2(100A_J) = 0$  to  $\phi_2(500A_J) = 0.5\phi_0$ . The fluxes of the adjacent pairs of splinter vortices match the complementarity condition at  $x \gtrsim 350A_J$ .

is used to obtain the phase pattern depicted in Fig. 4.

In Fig. 6 we show a phase pattern computed for the model dependence  $g(x) = 112.5 + 12.5 \times \sin(2\pi x/200A_J) + g_r(x)$ , where in addition to the smooth dependence (the second term) we add a term  $g_r(x)$ , which takes a certain random value for each of the facets and  $\langle g_r \rangle = 0$ . The plot shown in Fig. 6 obtained for the standard deviation  $\delta g_r = 5$  and  $l = 0.1A_J$ . It is seen from Figs. 5 and 6 that the random short-range variations of the lengths of the facets result in wiggling of the phase  $\varphi(x)$  with a wide range of length scales shorter than  $A_J$ . This wiggling effectively masks the splinter vortices carrying a small flux [1].

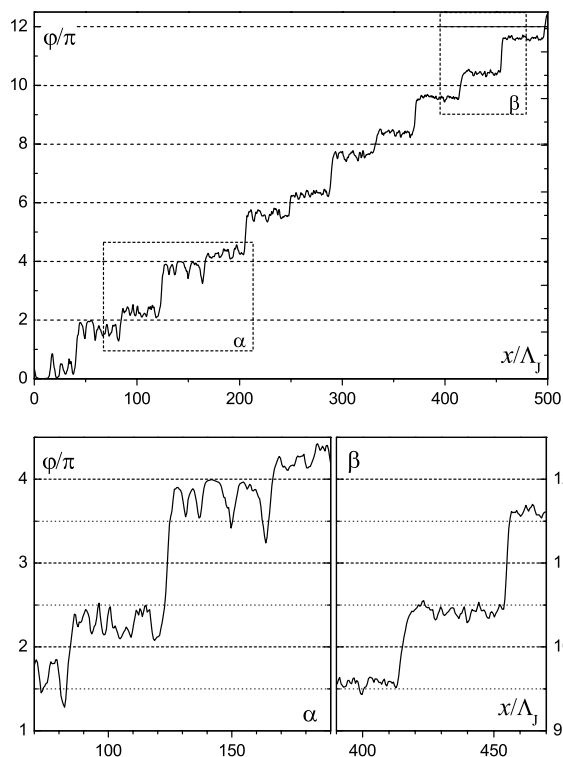


Fig. 5. The effect of random variations of the lengths of the facets on the phase pattern shown in Fig. 4.

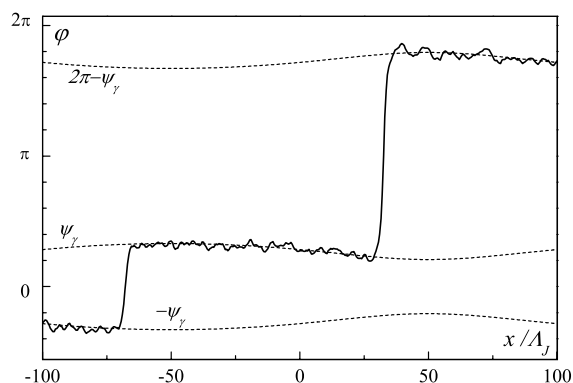


Fig. 6. The effect of random variations of the amplitude of the critical current density alternations on the phase pattern shown in Fig. 2.

#### 4. Summary

To summarize, we demonstrated that a smooth inhomogeneity of the Josephson properties of the

grain boundaries in YBCO thin films result in position dependent flux carried by the splinter vortices and thus to the complementarity condition breaking. The short-range inhomogeneities result in flux wiggling which can effectively mask the splinter vortices.

#### Acknowledgements

One of us (RGM) is grateful to J.R. Kirtley, V.G. Kogan, and J. Mannhart for useful and stimulating discussions. This research is supported by grant no. 2000-011 from the United States—Israel Binational Science Foundation (BSF), Jerusalem, Israel.

#### References

- [1] R.G. Mints, I. Papiashvili, J.R. Kirtley, H. Hilgenkamp, G. Hammerl, J. Mannhart, Phys. Rev. Lett. 89 (2002) 067004.
- [2] J. Mannhart, H. Hilgenkamp, B. Mayer, C. Gerber, J.R. Kirtley, K.A. Moler, M. Sigrist, Phys. Rev. Lett. 77 (1996) 2782.
- [3] R.G. Mints, Phys. Rev. B 57 (1998) 3221.
- [4] D.A. Wollman, D.J. Van Harlingen, D.J. Lee, W.C. Lee, D.M. Ginsberg, A.J. Leggett, Phys. Rev. Lett. 71 (1993) 2134.
- [5] P. Chaudhari, S.Y. Lin, Phys. Rev. Lett. 72 (1994) 1084.
- [6] C.C. Tsuei, J.R. Kirtley, C.C. Chi, L.S. Yu-Jhanes, A. Gupta, T. Shaw, J.Z. Sun, M.B. Ketchen, Phys. Rev. Lett. 73 (1994) 593.
- [7] D.A. Brawner, H.R. Ott, Phys. Rev. B 50 (1994) 6530.
- [8] J.H. Miller Jr, Q.Y. Ying, Z.G. Zou, N.Q. Fan, J.H. Xu, M.F. Davis, J.C. Wolfe, Phys. Rev. Lett. 74 (1995) 2347.
- [9] D.J. Van Harlingen, Rev. Mod. Phys. 67 (1995) 515.
- [10] D.B. Bailey, M. Sigrist, R.B. Laughlin, Phys. Rev. B 55 (1997) 15239.
- [11] M. Sigrist, Prog. Theor. Phys. 99 (1998) 899.
- [12] C.C. Tsuei, J.R. Kirtley, Rev. Mod. Phys. 72 (2000) 969.
- [13] C.L. Jia, B. Kabius, K. Urban, K. Herrmann, J. Schubert, W. Zander, A.I. Braginski, Physica C 196 (1992) 211.
- [14] S.J. Rosner, K. Char, G. Zaharchuk, Appl. Phys. Lett. 60 (1992) 1010.
- [15] C. Træholt, J.G. Wen, H.W. Zandbergen, Y. Shen, J.W.M. Hilgenkamp, Physica C 230 (1994) 425.
- [16] H. Hilgenkamp, J. Mannhart, Rev. Mod. Phys. 74 (2002) 485.

- [17] H. Hilgenkamp, J. Mannhart, B. Mayer, *Phys. Rev. B* 53 (1996) 14586.
- [18] H.J.H. Smilde, A. Ariando, D.H.A. Blank, G.J. Gerritsma, H. Hilgenkamp, H. Rogalla, *Phys. Rev. Lett.* 88 (2002) 057004.
- [19] A brief summary of this work was presented at the 23rd International Conference on Low Temperature Physics (LT23); R.G. Mints, I. Papiashvili, *Physica C* vol. 388–389 (2003) 713.
- [20] L.D. Landau, E.M. Lifshitz, *Mechanics*, Pergamon Press, Oxford, 1994, p. 93.
- [21] N. Bogolubov, Y. Mitropolsky, *Asymptotic methods in the theory of non-linear oscillations*, 2nd ed., Hindustan Pub., Delhi, India, 1961.